CRACKING AND EDGE-LOADING EFFECTS ON STRESSES AND DEFLECTIONS IN A SOIL-CEMENT PAVEMENT

Per E. Fossberg, International Bank for Reconstruction and Development; and
James K. Mitchell and Carl L. Monismith,
Institute of Transportation and Traffic Engineering, University of California, Berkeley

Two 8½-in. thick panels of stiff soil-cement base were constructed on a soft clay subgrade, and one of them was loaded to crack. Both pavements were then tested in repeated loading, unsurfaced and surfaced with 1, 3, and 5 in. of asphalt concrete. Deflections, stresses, and strains under loading were recorded and compared. Vertical deflections were greater by about 20 percent, and subgrade stresses directly under the load were greater by at least 50 percent in the cracked section than in the uncracked pavement. Cracking had a large influence on horizontal strains near the crack in the base but had only a small influence on strains in the asphalt concrete surfacing. A saw-cut was made through the uncracked pavement surfaced with 5 in. of asphalt concrete, and repeated plate-load tests were done with the plate center 24 and 8 in. from the cut. Loading at 24 in. had negligible effects on vertical deflections but increased subgrade stresses near the cut by about 40 percent. Loading at 8 in. increased vertical deflections by at least 60 percent and subgrade stresses near the cut by about 100 percent. Laboratory-determined values for the elastic properties of the clay, the soil-cement, and the asphalt concrete and the various assumed loading conditions were used as input for computer predictions of stresses and deflections. Very satisfactory agreement was obtained between the predicted and measured stresses and deflections.

•EXPERIENCE and theoretical investigations have shown that most soil-cement pavements are subject to cracking due to shrinkage stresses during curing, traffic loadings, and temperature stresses. Although it has long been realized that cracking in soil-cement bases is likely to be the rule rather than the exception, recent studies have been aimed at the explanation of crack development, and some study has been made of techniques for minimizing crack formation (2, 3, 4). Little is known, however, about the relative performance of cracked and uncracked soil-cement slabs under load.

During a recent investigation at the University of California, Berkeley (1), the opportunity arose to carry out field measurements of stresses and deformations associated with edge loading and cracking of a soil-cement pavement. A recently developed finite-element program, capable of 3-dimensional analysis (5, 7), provided a tool for analytical treatment of the problem and thus allowed for correlation to be drawn between field measurements and theoretical analysis.

This paper gives an outline of the study, reports on field test results, describes the method of analysis, compares the results of the theoretical analyses with field data, and draws conclusions relative to the design and performance of soil-cement pavements.

OUTLINE OF STUDY

Two panels of soil-cement base (cement-treated granular material meeting Portland Cement Association's criteria for wet-dry and freeze-thaw testing) were constructed, each approximately 8.5 in. thick and 20 ft square in plan on top of a natural clay subgrade. Classification properties of the subgrade clay are as follows:

Property	Value
Yellow plastic clay	
Water content, percent	18 to 30
Liquid limit, percent	56
Plasticity index, percent	34
Dry density, lb/ft^3	92 to 102
CBR	2 to 5
Unconfined compressive strength, psi	10 to 50

A cement content of 5.5 percent and well-graded gravel with fines were used in the soil-cement as follows:

Sieve Size	Percent Finer by Weight
¾ in.	100
No. 4	62
No. 16	39
No. 50	25
No. 200	17

One of the two pavement sections was loaded until it cracked. On top of the base, 5 in. of asphalt concrete surfacing was constructed in 3 lifts, permitting determination of the influence of asphalt concrete thickness on the performance of the pavement sections with both cracked (pavement 1) and uncracked (pavement 2) soil-cement base.

Repeated-load plate tests (20 load applications per minute of 0.1-sec duration) were carried out. On the subgrade, plate diameters of 24 in. and 30 in. with pressures up to 5 psi were used. On the soil-cement base and the successive lifts of asphalt concrete, the plate sizes ranged from 8 to 24 in. in diameter with plate pressures from 2.5 to 150 psi, depending on plate size. For each repeated-load plate test, vertical deflections at the pavement surface, at the surfacing-base and base-subgrade interfaces, and at various depths into the subgrade were measured. Vertical stresses and horizontal strains were measured at various locations in the subgrade, soil-cement base, and asphalt concrete surfacing of both pavement structures. Figure 1 shows the location of the gauges in the pavement structure. A complete description of the instrumentation and test procedures is given elsewhere (1).

As a final test on the uncracked pavement, after the full 5 in. of asphalt concrete had been placed and the load tests completed, the pavement was cut with a diamond saw over its full length and full depth of surfacing and base. Repeated-loading tests were then carried out with the center of the plate 24 in. (position A, Fig. 1) and 8 in. (position B) from the cut. This arrangement permitted study of edge loading in an instrumented part of the pavement. Figure 1 shows the position of the saw cut in pavement 2 and the position of the crack in pavement 1.

Laboratory tests were used to ascertain the elasticity and strength characteristics of the pavement materials. The tests were done on cylindrical samples of undisturbed subgrade clay, on soil-cement beams, on cylinders and prisms prepared in the laboratory or cut from the test pavements, and on beams and prisms of asphalt concrete also cut from the test pavements. A triaxial apparatus, allowing for independent application of axial and radial stresses, was used to test the clay and soil-cement cylinders. For the subgrade cylinders and some of the soil-cement specimens, strains were recorded with linear variable differential transformers (LVDT); for the asphalt concrete and other soil-cement specimens, bonded strain gauges were utilized. For all tests, the load frequency and duration were the same as those used for the repeated-load plate tests on the prototype pavements.

Laboratory data used in the theoretical analyses were determined to correspond to the appropriate field conditions, e.g., subgrade moisture content, soil-cement curing

time, and asphalt concrete temperature. On this basis the following values were selected (Fig. 2):

1. The subgrade was nearly saturated but with water content varying with depth as shown in Figure 2, Poisson's ratio was assumed to be 0.48, and the elastic modulus varied between 1,600 and 18,000 psi;
2. Field testing was started on the soil-cement base approximately 6 weeks after construction at which time the elastic modulus had reached a relatively constant value of 2,800,000 psi and Poisson's ratio was determined to be 0.16; and
3. The asphalt concrete temperature was comparatively uniform—65 F—for all the field tests at which Poisson's ratio was taken to be 0.35 and the elastic modulus was 350,000 psi.

FIELD TEST RESULTS

Cracking of Soil-Cement Base

On the basis of recorded tangential and radial strains in the base, it was postulated that the position of the crack caused by overloading was approximately as shown in Figure 1. Figure 3a shows the radial strains close to the top (gauge 2-6) and the bottom (gauge 2-8) of the unsurfaced soil-cement slab and at a horizontal distance of 3 in. from the center of the load plotted as a function of plate load and pressure. For the 8-in. diameter plate, the load-strain relationship recorded on gauge 2-8 was close to linear and of about the same magnitude as found for the uncracked slab. For the 12-in. and 16-in. diameter plates, however, a drastic increase in strains was recorded on gauge 2-8, indicating cracking under the 12-in. plate load. (After cracking had occurred the "strain" recorded on the LVDT type of strain gauge mainly reflects the gap at the crack. Thus, a recorded strain of 160×10^{-6} on a gauge where the anchor plates are 2 in. apart represents a gap of about 320×10^{-6} in.)

The plate size appears to be of little significance for the induced strain, the determining factor being plate load. Gauge 2-6 showed that, for the 12-in. diameter plate, tensile strains occurred even at a depth of 1½ in. below the top of the pavement. This may be taken as a further indication of the position of the crack.

The data shown in Figure 3a have been replotted in terms of a profile through the soil-cement slab (Fig. 4). The large difference in strains at the bottom of the base, as recorded under the 8-in. diameter plate (base uncracked) and the 12-and 16-in. diameter plates (base cracked), is evident.

Figure 3b shows tangential strains close to the top (gauge 2-5) and the bottom (gauge 2-7) of the soil-cement slab, 6 in. from the center of the load, and in a direction nearly parallel to the apparent direction of the crack. From the load-strain patterns observed for the 8-in. diameter plate (compression near top, tension near bottom), zero tangential strains would occur about midheight in the uncracked slab. For the cracked slab, in the direction of gauges 2-5 and 2-7, the data for the 12-and 16-in. diameter plates show that this pattern remains essentially unchanged, although the strains are somewhat larger for the cracked slab. Had the slab remained uncracked for the 12-in. and 16-in. diameter test plates, the strains should have been somewhat less than those recorded for the 8-in. plate for a given plate load. The data shown in Figure 3b indicate that the strains in the positions of gauges 2-5 and 2-7 have increased by at least 20 percent because of the cracking. This increase is important because the tensile stresses at the bottom of the slab, near the crack, and in a direction parallel to it may be critical for the propagation of further load-associated cracking.

Vertical deflections under repeated loading are shown in Figure 5. For the 8-in. diameter test plate, when the slab was not cracked, the load-deflection relation is close to that shown for the uncracked slab. However, for the cracked slab subjected to repeated loading on 12- and 16-in. diameter plates, deflections are increased. Based on argument in the preceding paragraph, Figure 5 shows that cracking of the pavement causes an increase in deflection of at least 20 percent. The increases postulated for tangential strains at positions 2-5 and 2-7, and for the vertical deflections, are thus in a agreement.

Figure 1. Positions of stress and strain gauges, crack and pavement cut, and loads A and B.

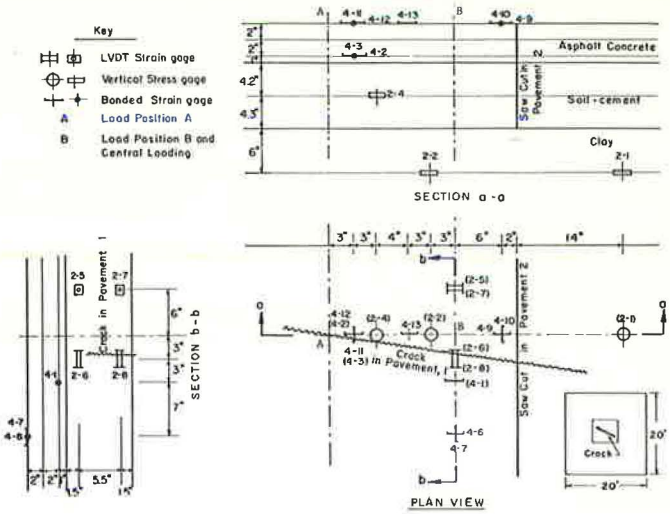

Figure 2. Property values used for structural analysis of pavement.

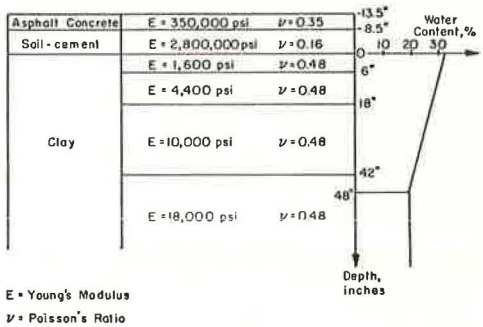

Figure 3. Resilient strains under repeated loading of unsurfaced, cracked soil-cement pavement near top and bottom.

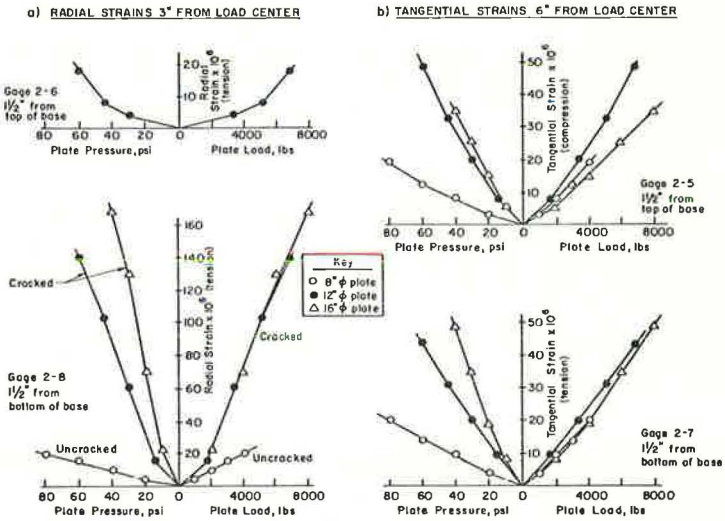

Figure 4. Resilient radial strains under repeated loading of unsurfaced, cracked soil-cement pavement at 3-in. distance from center of load.

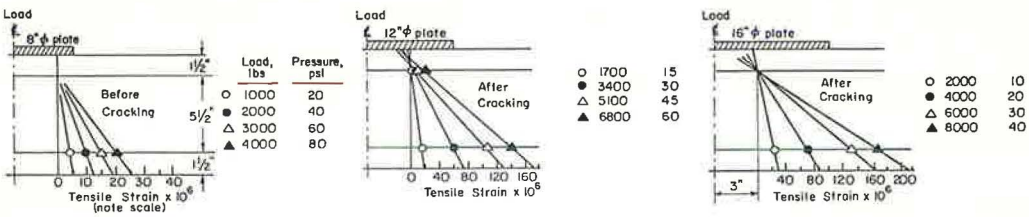

Figure 6 shows the vertical stresses obtained for gauges 2-1 and 2-2 installed 6 in. beneath the top of the subgrade and at horizontal distances of 22 and 3 in. respectively from the center of the loaded area. It will be noted that for gauge 2-1 the stresses were of the same magnitude as reported for the uncracked slab. For gauge 2-2, however, which was situated close to the center of the load and presumably close to the crack, the cracking seemed to have a more profound effect. Although the stresses before cracking (8-in. diameter test plate) are about equal to those obtained for the uncracked slab, cracking caused a sharp increase in stress at the position of gauge 2-2. It appears that the subgrade stresses near the crack increased by at least 50 percent as a result of cracking of the slab, based on the values recorded for the 12- and 16-in. diameter plates.

For both the cracked and the uncracked pavements, the provision of 5 in. of asphalt concrete surfacing reduced the base deflection and subgrade stresses by only about 20 percent. This relatively small effect can probably be attributed to the fact that the asphalt concrete in this experiment had a stiffness only about one-eighth of that of the soil-cement. The asphalt concrete had, however, a large effect in reducing the vertical stresses at mid-depth in the base. Cracking of the base had a large influence on horizontal strains near the crack in the base but had only a small influence on strains in the asphalt concrete surfacing.

Edge Loading

Repeated loading was carried out on the sawed pavement by using 8-, 12-, and 18-in. diameter plates with the centers located 24 and 8 in. from the cut (load positions A and B respectively shown in Fig. 1). The saw cut was made near the end of the test program after tests were made of the completed pavement structure containing a 5-in. thick asphalt concrete surfacing.

Figure 7 shows the deflection patterns under a 12-in. diameter plate at load positions A and B. Although the deflection was considerably increased when the loading was close to the edge, the difference is accounted for mainly in the deformation of the upper 1 ft of the subgrade. For load position A, the maximum deflection occurred under the load and not at the edge. This is contrary to what one might have expected, considering the high stiffness of the soil-cement base. An interesting observation is that the soil-cement slab on the other side of the cut also deflected somewhat. There is no doubt that the saw cut extended right through the pavement; hence, the observed deflection of the adjacent slab must have been due to the subgrade "pulling" it down. This again was unexpected in view of the high slab stiffness and the absence of load transfer across the cut.

The deflections of the base course under the center of the load, as functions of plate size, pressure, and load are shown in Figure 8 for load positions A and B. In both cases, the deflections were closely related to the plate load, irrespective of plate size, a finding in agreement with the cases of central loading of the slab. Conversely, the deflections increased rapidly with plate size for any given pressure intensity on the plate. Loading at position A gave deflections only slightly larger than those at central loading, and loading at position B gave deflections at least 50 percent larger. A tentative conclusion is, therefore, that for a soil-cement pavement loading 2 ft or more from the edge can be treated as central loading and loading very close to the edge may cause considerably larger deflections and also higher stresses and strains in the base.

Figure 9a shows the stresses in the clay subgrade (gauge 2-2) as a function of the plate size, pressure, and load for test position A; Figure 9b shows the same data for test position B. As in the case of deflections, the stresses in both cases were uniquely related to the plate load, irrespective of plate size. A comparison of these load-stress diagrams with values for central loading shows that the stresses obtained by central loading were increased by approximately 40 percent and 100 percent for load positions A and B respectively.

Figure 10 shows the load-strain data for 4 of the 10 gauges positioned on top of the various asphalt concrete lifts. In these diagrams, the full and dashed lines represent load positions A and B respectively. In the following, some of the most significant aspects will be discussed.

Figure 5. Resilient vertical deflections as function of plate size, plate pressure, and plate load for cracked and uncracked pavements.

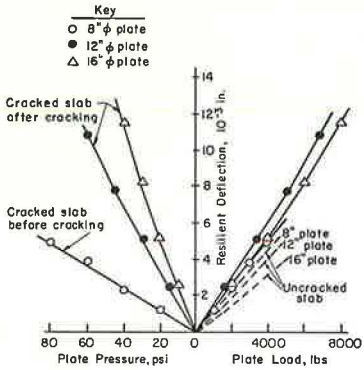

Figure 6. Vertical stresses at 6-in. depth into subgrade.

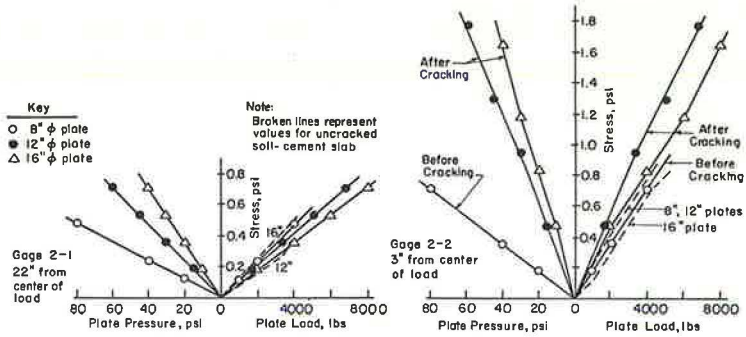

Figure 7. Effect of curing temperature on strength and failure strain in both tension and compression.

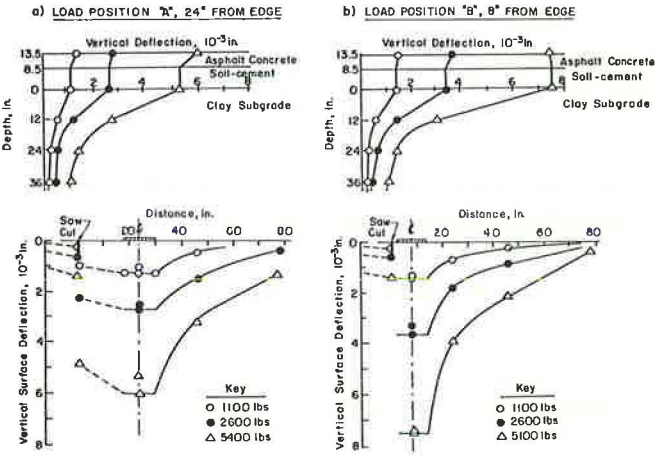

Figure 8. Resilient vertical deflections at top of soil-cement base under repeated loading on edge of pavement with 5-in. asphalt concrete surfacing.

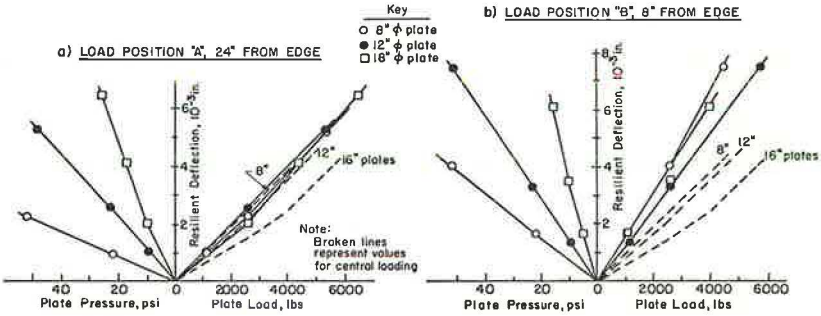

Figure 9. Vertical stresses in subgrade under repeated loading on edge of pavement with 5-in. asphalt concrete surfacing.

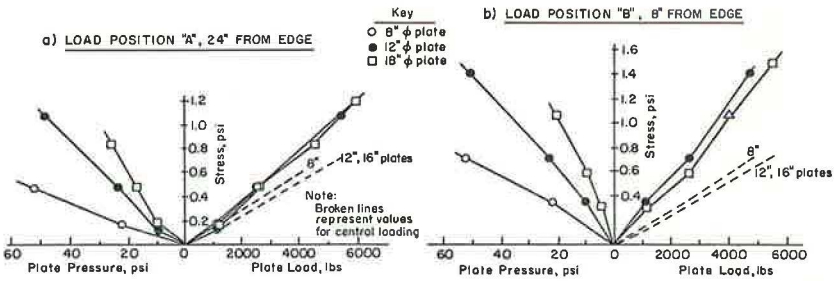

On gauge 4-1 compressive strains were observed when the load was at position A. Good agreement is obtained between these strains and those obtained in the central loading case for gauge 4-2 in about the same position relative to the load. (The inflection points of the deflection basin under central loading of this pavement system lie on a circle with a radius of approximately 2 ft. Thus, for loading 2 ft from the edge, which is position A, strains recorded in the vicinity of the load should be comparable with those obtained in the central loading case.) In the present case, the strains are relatively little affected by the plate size. From the geometry of the loading (Fig. 1) it is entirely logical that relatively large tensile strains should be recorded on this gauge when the load is at position B. The data shown in Figure 10 indicate that this is correct. Although the changes in strains from compression to tension, depending on load position, are important when fatigue is considered, the stresses resulting from the strains here encountered are not critical for the asphalt concrete.

On gauge 4-3, with the load at position A, relatively small compressive strains were recorded for the 12- and 18-in. diameter plates, and no strains were recorded under the 8-in. plate. The position of this gauge (tangentially 3 in. from the center of the load) was comparable to that of gauge 4-1 in the case of a central loading (6 in. from the load). Relatively good agreement was found to exist between strains recorded in the two cases. When tests were made at position B, higher compressive strains were recorded. Because this strain was measured in a direction parallel to and relatively far from the edge and tangential to the load, one may expect a relatively close agreement with the readings for the same gauge under central loading. A comparison with the data for gauge 4-3 under central loading shows excellent agreement.

Gauge 4-7 recorded compressive strains at both edge load positions. As expected, the largest strains were experienced for load position B, this being the more severe loading condition and the one where the load was the closer to the gauge. With the load 8 in. from the edge, strains 2-3 times larger than those of the central loading case were measured.

On gauge 4-11, compressive strains were recorded at load position A. For load position B, strain recordings were only obtained for the 18-in. diameter plate. Although these strains were smaller than those recorded by the same gauge with the load at position A, they were slightly larger than those recorded by the gauge in the same position relative to a central load, which is to be expected. Furthermore, for load position B, the strains recorded on gauges 4-11 and 4-3 were about equal, which is reasonable according to the geometry shown in Figure 1.

METHOD OF ANALYSIS

Explicit solutions for 2- and 3-layered pavement systems and computer solutions based on multiple-layer theory and on finite-element systems are readily available for the theoretical analysis of axisymmetric (central) loading of pavements. Although these solutions are not directly applicable to the analysis of loading near a pavement edge or a crack, recent developments in finite-element analysis make it possible to also treat these cases of loading analytically.

Wilson (7) developed a finite-element computer program for a 3-dimensional prismatic solid. This program, which was adapted for pavements by Pretorius (5), was used in the present study to evaluate the effects of traffic loads close to the pavement edge. A transverse section of the structure illustrating the configuration of the finite elements (each element representing a longitudinal prism) is shown in Figure 11. Although the element properties could be varied at will in the transverse plane (limited, however, to 12 linearly elastic material types), these properties remain constant along the prisms in the longitudinal direction.

The system is essentially 2-dimensional, with the third dimension introduced into the idealized structure by expressing the load as a Fourier series in this direction. Stresses and deformations caused by each Fourier term are summed, and the process is continued until further additions become insignificant. The number of Fourier terms required increases with the ratio between the "longitudinal distance between planes of symmetry" (where the loads are applied) and the "loaded length." For a stiff pavement,

Figure 10. Resilient strains in asphalt concrete under repeated loading on edge of pavement with 5-in. asphalt concrete surfacing (load and gauge positions as shown in Fig. 1).

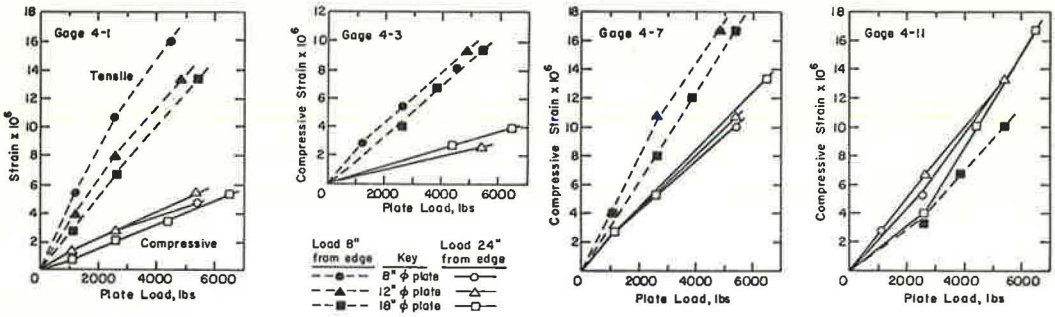

Figure 11. Finite-element mesh used for edge-loading conditions.

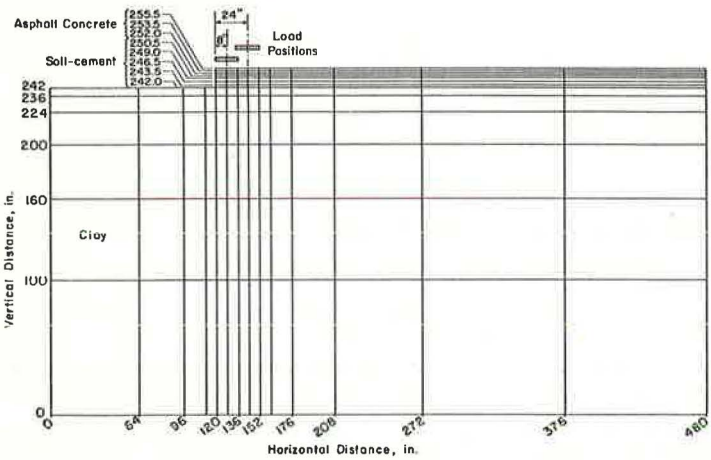

Figure 12. Finite-element mesh in vicinity of crack for plane-symmetric loading.

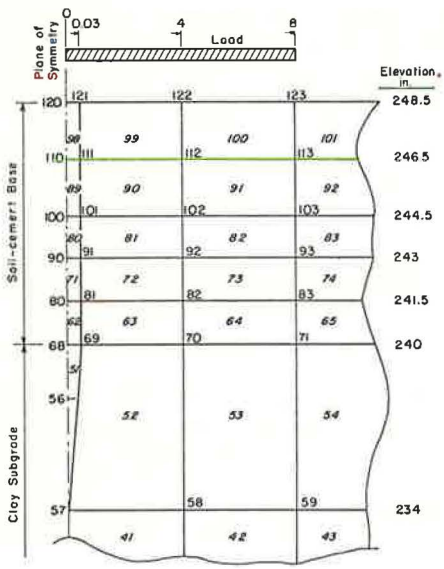

the distance between loads has to be large to avoid mutual interference, yet the loaded length has to be commensurate with the size of the loading plates. In the present study, the distance between planes of symmetry was chosen to be 240 in., and the plate size was 16 by 16 in. (corresponding to an 18-in. diameter circular plate). For these conditions 16 Fourier terms were required to obtain the desired accuracy. For the finite-element grid shown, each Fourier term required nearly 2 minutes of time on a CDC 6400 computer; hence, the complete solution took approximately half an hour. For this reason, only 2 solutions were obtained, viz., with the load center 8 in. and 24 in. from the pavement edge.

The same computer program was used to analyze stresses and deformations in the cracked soil-cement pavement. The configuration of elements used near the cracked zone is shown in Figure 12. It was assumed that the crack passed through the centerline of the loaded area. In this way, the plane of the crack acted as a plane of symmetry, and only the system on one side of the crack needed to be analyzed. This represents a less severe condition than if the total load were concentrated on one side of the crack. However, when one considers that shear stresses can be transmitted through the cracked zone, and also the likely position of the crack as shown in Figure 1, the assumed system appeared reasonable.

The finite-element grid shown in Figure 12 extends to the same depth as the grid shown in Figure 11. In the horizontal direction the subgrade extends to 240 in. and the soil-cement base extends to 120 in. from the crack, thus simulating the actual dimensions of the pavement prototype. The analysis was based on loading a 16-in. square plate and a distance between planes of symmetry of 240 in. in the longitudinal direction.

The field observations indicated that the crack caused by overloading the plate did not extend to the surface of the base. This would be expected because, even for the cracked base, the uppermost part will be subjected to horizontal compressive bending stresses. One may rationalize, therefore, that, once the base cracks in flexural tension (i.e., when the tensile stress reaches the tensile strength), the crack will propagate upward to the point where the tensile stress falls below the tensile strength. The extent of the crack propagation can be determined by analyzing the stress conditions for various crack depths. In the finite-element grid shown in Figure 12 provision was made for this procedure in that a narrow column of elements adjacent to the crack could be assigned various elastic properties. For the uncracked pavement, the narrow elements were assigned the same elastic properties as the adjacent elements. Then, assuming a crack propagating upward, we consecutively assigned elements 62, 71, 80, and 89 a very low elastic modulus (1 psi) to reflect the cracked condition.

RESULTS OF PAVEMENT ANALYSES

Cracking of Soil-Cement Base

Analyses were based on the assumption that cracks extended upward from the bottom of the soil-cement 0, 1½, 3, 4½, and 6½ in. The assumed loading was 6,400 lb on a 16-in. square plate (corresponding to an 18-in. diameter circular plate). The results of these analyses are shown in Figure 13a. In the uncracked condition the maximum tensile stress is approximately 100 psi. If a crack is initiated at this stress (i.e., if the tensile strength is 100 psi), stress concentration at the end of the crack will cause the crack to propagate. Thus, for upward crack propagations of 1½ and 3 in. the maximum tensile stress will be at least 120 psi and 140 psi respectively as shown in Figure 13a. Once the crack rises to 4½ in., a reduction of the maximum tensile stress (at the end of the crack) is evident, although it is still likely to be well above 100 psi. However, had a crack risen 6½ in. above the bottom of the slab, the computer solution indicates that only compressive stresses would occur. This may not be quite so, however, because the compressive stress indicated (40 psi) is an average of the stresses over the uncracked top 2 in. of the slab (element 98, Fig. 12). Thus, because the maximum horizontal compressive stress at the top of the element is likely to exceed 80 psi, it is likely that tensile stresses will still occur at the bottom of the element. This tensile stress is not likely to reach 100 psi, so one may assume that at

least the upper 2 in. of the pavement would remain uncracked. It should be borne in mind, however, that, because of the characteristic stress singularity at the crack tip, the finite-element solution may not be valid in this region. Hence, the stresses computed for the crack tip may be in error. A general conclusion of this analysis is, nevertheless, that, for materials and geometric conditions similar to those in this experiment, a crack in a soil-cement slab once initiated in bending is likely to extend upward some ⅔ to ¾ of the slab thickness. Such cracks once initiated in bending may ultimately extend over the full depth because of thermal and shrinkage stresses inasmuch as shrinkage and thermal cracks originate at the top surface and propagate downward.

Figure 13b shows the horizontal stresses 6 in. from the crack. As expected, a stress relaxation develops, particularly in the lower part of the slab with upward propagation of the crack. Thus, for a 6½-in. crack height, the maximum stresses at top and bottom are approximately ⅔ and ⅓ respectively of the stresses in the uncracked slab. It is noteworthy that the neutral axis stays close to the middle of the slab, even for the cracked pavement.

Figure 14a shows the crack openings calculated for various hypothetical crack depths. For a crack depth of ⅔ to ¾ of the slab thickness, a maximum crack opening of about 7 to 8 × 10^{-4} in. can be expected under the given load of 6,400 lb on a 16-in. square plate. Comparing the calculated crack opening with the field strain gauge observation (in terms of linear displacement of end platens in the LVDT type of strain gauge), we note that the field value is less than predicted. One reason for the discrepancy may be that the crack does not ideally "intersect" the gauge as assumed for the computation. The same kind of discrepancy was noted by George (4), who attributed it to viscous effects in soil-cement.

Figure 14b shows the horizontal strains in the soil-cement slab above the cracked zone for various crack depths. This diagram is in agreement with the one shown in Figure 13 for the horizontal stresses and confirms that for a crack depth of 6½ in. a slight tension will occur at the bottom of the upper 2-in. element. Good agreement is observed between the calculated strains and the field data.

Figure 15 shows vertical stresses at a 3-in. depth into the subgrade in a plane perpendicular to the plane of the crack (Fig. 15a) and in a plane parallel to and 6 in. away from the crack (Fig. 15b). Figure 15a shows that a 4½-in. crack will increase the maximum vertical stress by about 30 percent above the uncracked condition and a 6½-in. crack will increase it by about 50 percent. The latter percentage corresponds to the figure calculated on the basis of field data. Stresses observed on gauge 2-2 for loading on 12- and 16-in. diameter plates are shown in Figure 15a at about the position the gauge would have according to the crack position shown in Figure 1. We note that, although the stress recorded on gauge 2-2 for loading on a 16-in. diameter plate is less than that predicted for the cracked slab, the recorded stress for the 12-in. diameter plate is close to the predicted value.

For a plane 6 in. away from the crack, Figure 15b shows less variation in stress with crack depth than does Figure 15a for positions close to the load. Stresses observed on gauge 2-1 are shown in Figure 15b, again at about the position the gauge would have according to the position shown in Figure 1. The agreement is reasonable if the speculative nature of the positioning of the crack in relation to the gauge is considered.

Figure 16 shows the deflection patterns for the slab with cracks of different depths. The curves show relatively good agreement with the subgrade stress patterns shown in Figure 15a. From data shown in Figure 16 we can deduce that a 6½-in. crack increases the vertical deflection about 20 percent above that for the uncracked slab. This again is supported by the field observations.

Edge Loading

At both edge-loading positions A and B, 8-, 12-, and 18-in. diameter plates were used. For the computer solutions for the 2 test positions, however, only 1 plate size, 16 in. square (or 18-in. diameter), was analyzed because of the large amount of computer time required to solve the edge-loading problem.

Figure 13. Finite-element solutions for horizontal stresses in plane of tension crack and 6 in. away as functions of level of cracking of 8½-in. thick soil cement slab under 6,400-lb load on 16- by 16-in. square plate.

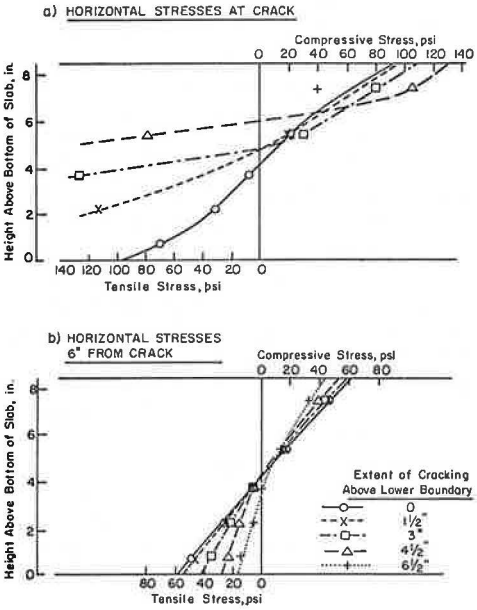

Figure 14. Finite-element solutions for crack opening and horizontal strains in uncracked portion as functions of extent of cracking of 8½-in. thick soil-cement slab under 6,400-lb load on 16- by 16-in. square plate.

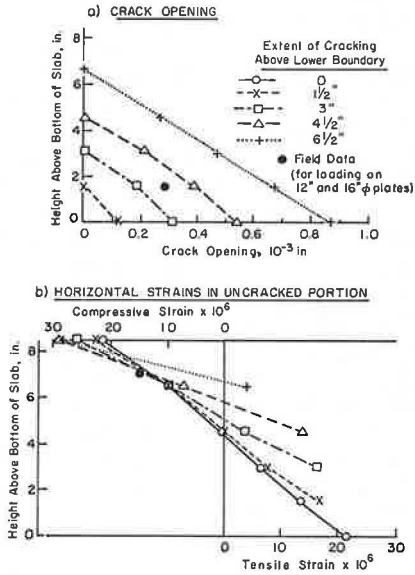

Figure 15. Finite-element solutions for vertical stresses at 3-in. depth in subgrade under cracked soil-cement slab and under 6,400-lb load on a 16- by 16-in. square plate.

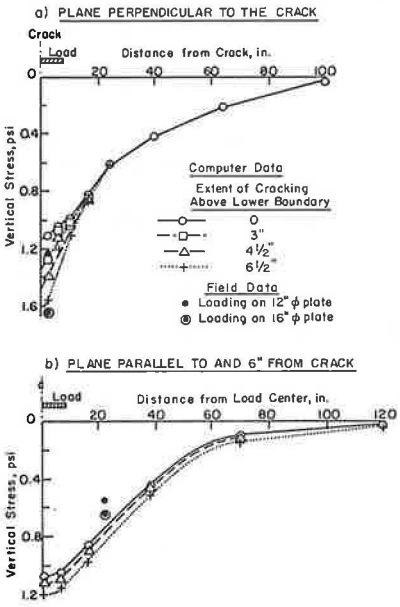

Figure 16. Finite-element solutions for deflections at various distances from tension crack in 8½-in. thick soil-cement slab as functions of extent of cracking above lower boundary under 6,400-lb load on a 16- by 16-in. square plate.

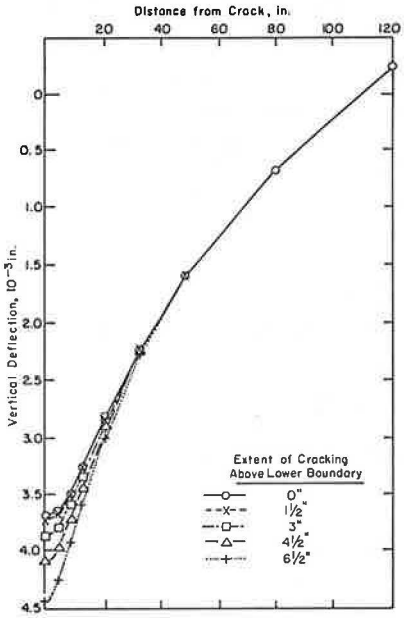

Figure 17 shows a comparison of field data and computed predictions for vertical deflections of the pavement under edge loading. Loading 24 in. and 8 in. from the edge gave computed deflections approximately 10 and 80 percent respectively above those computed for the central loading case. These percentages are somewhat higher than the corresponding field observations. The relative magnitudes of the edge-loading deflections, with the value being about 70 percent larger at position B than at position A, represent a ratio somewhat larger than that for the field data. The predictions underestimate the actual plate deflections by approximately 15 percent.

Figure 18 shows the deflection patterns with horizontal and vertical distance from the pavement edge for loading positions A and B respectively. The agreement between observed and calculated deflections is very good. Vertical stresses were recorded at 2 isolated points: at mid-depth in the base and at 6-in. depth within the subgrade. The results of the computer predictions, not reproduced here, show a satisfactory agreement between measured and predicted values for both loading positions A and B.

Figure 19 compares observed and predicted horizontal strains in the surfacing and base in a plane perpendicular to the pavement edge for loading position B. The upper diagram shows strains in the plane of the drawing, and the lower diagram shows strains in a direction perpendicular to that plane, i. e., in a plane parallel to the pavement edge. The strains are plotted along a vertical line 21 in. in from the edge of the pavement. A good agreement exists between recorded and predicted strains in the plane perpendicular to the edge (Fig. 19a). In the direction parallel to the edge (Fig. 19b), however, predicted strains are considerably larger than the recorded.

Figure 20 shows strains along a plane parallel to and 8 in. from the pavement edge for load position B (also 8 in. from the edge). The upper diagram shows horizontal strains in this plane, and the lower diagram shows the strains in a direction perpendicular to that plane. A fairly good agreement exists between the observed and the predicted values.

The following 2 important considerations from data shown in Figures 19 and 20 are applicable both to the edge-loading case and to the situation in a cracked pavement with a load approaching the crack:

1. Figure 20a confirms that for load position B critical tensile strains occur at the bottom of the soil-cement slab near the crack in the direction parallel to the crack. For the edge-loading case, which is also closely applicable for a wide shrinkage crack with little or no load transfer across the crack, this strain is some 40 to 50 percent higher than that observed in the uncracked slab (full line, Fig. 14b). Also, for the case of a "closed" crack the field experiment indicated an increase in these critical strains of about 20 percent above those for the uncracked slab (Fig. 3b). In both cases, therefore, there is a real danger that further cracking will propagate in the direction perpendicular to the existing crack; this in turn will lead to corner-loading situations in the areas adjacent to the cracks, causing further serious tensile stress conditions at the top of the base and surfacing.

2. The computer solutions confirm the recording on gauge 4-1 (Fig. 10) that, as the load approaches the crack, there is a reversal of the horizontal strains in the direction perpendicular to the crack (x-direction) in the top of the base and surfacing from compressive for load position A (not shown) to tensile for load position B (Fig. 19a). Reversal of strains from tensile to compressive also occurs at the bottom of the soil-cement slab as the load approaches the crack. As far as the soil-cement base is concerned, none of these strains is as severe as those referred to in the preceding paragraph. However, they increase in significance when the fatigue aspects of stress reversals is considered.

The two strain situations described form a sufficient rationale for formation of the well-known "ladder" cracking in the wheelpaths of pavements with cement-stabilized bases. An excellent treatise on this subject has been given by Pretorius (6).

CONCLUSIONS

The present study has demonstrated a good agreement between field observations and theoretically determined stresses and deformations associated with cracking and

Figure 17. Predicted and observed deflections at top of base for loading 8 and 24 in. from pavement edge.

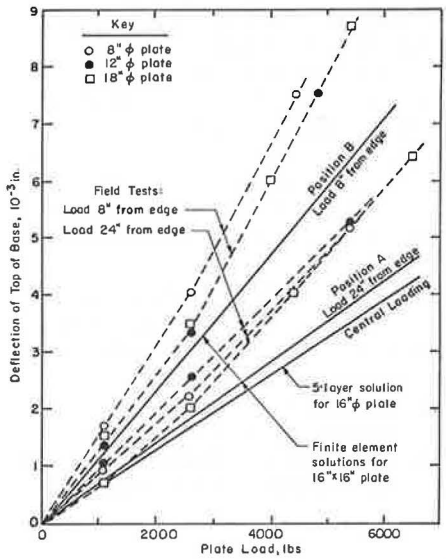

Figure 18. Vertical deflection patterns for 6,400-lb edge load on 16-in. square plate.

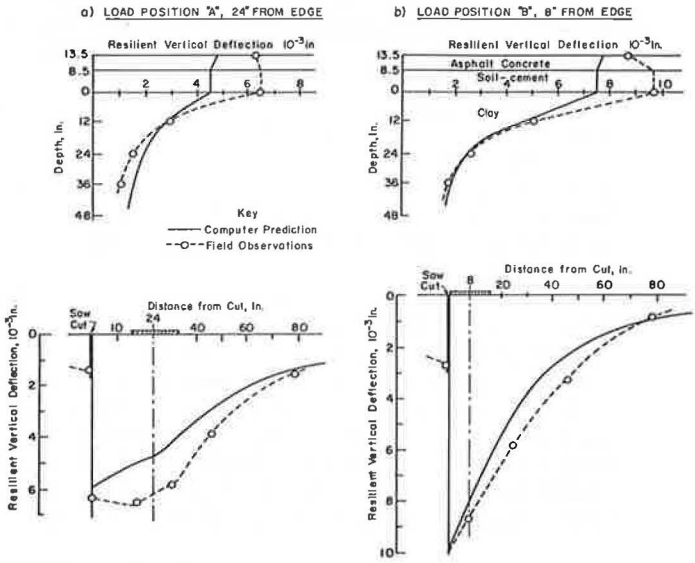

Figure 19. Horizontal strains in plane perpendicular to pavement edge under 6,400-lb loading on 16-in. square plate 8 in. from pavement edge.

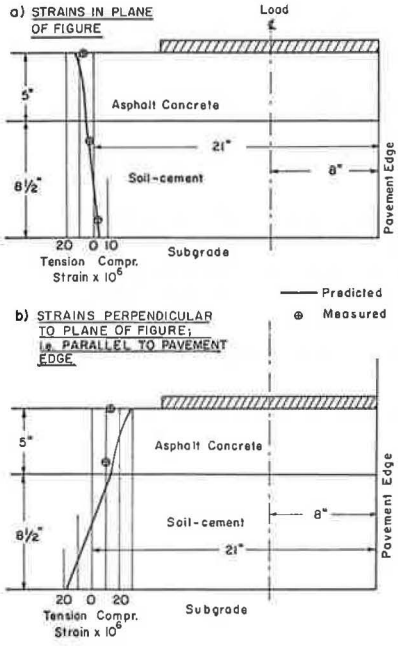

Figure 20. Horizontal strains in plane parallel to and 8 in. from pavement edge under 6,400-lb load on 16-in. square plate 8 in. from pavement edge.

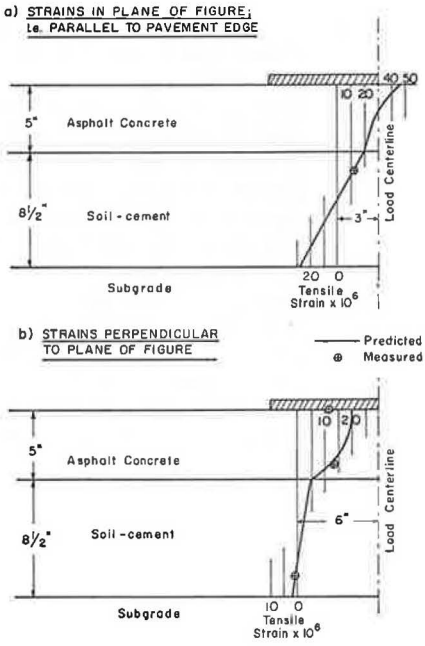

edge loading of a soil-cement pavement. The following specific conclusions can be drawn:

1. Cracking of a soil-cement pavement under loading only slightly increased (about 20 percent) vertical deflections but substantially increased (about 50 percent) vertical stresses in the subgrade near the crack when the load was placed directly over the crack. Cracking had a large influence on horizontal deformations near the crack. These data suggest that, within the reasonable range of experimental error, deflection measurements cannot be used to detect cracking of a soil-cement pavement.
2. The investigations on edge loading showed that, for the pavement structure tested in this study, loading at least 2 ft from the pavement edge can be analyzed as "central loading." Loading close to the edge is more severe in terms of stresses and deformations in both base and subgrade, however; and this should be taken account of in the pavement design.
3. Traffic loading of a soil-cement pavement where initial cracking has occurred (because of shrinkage or traffic and temperature stresses or all of these) causes critical tensile stresses and stress reversals that can explain the formation of the typical "ladder" cracking in the wheelpaths of such pavements.
4. The stiffness of an asphalt-bound layer placed on top of a layer of soil-cement has an influence on the stresses in the soil-cement layer and the deflection of the pavement structure. In this investigation 5 in. of asphalt concrete whose stiffness under the conditions of test was only about 12 percent of the soil-cement exerted a comparatively small influence on the response of the structure to load.

ACKNOWLEDGMENTS

The investigations described in this paper were made possible through a grant from the Portland Cement Association. The authors are pleased to acknowledge both this support and the helpful discussions and encouragement provided by B. E. Colley and Peter J. Nussbaum of that organization.

REFERENCES

1. Fossberg, P. E. Load-Deformation Characteristics of Three-Layer Pavements Containing Cement-Stabilized Base. Univ. of California, Berkeley, PhD dissertation, 1970.
2. George, K. P. Shrinkage Characteristics of Soil-Cement Mixtures. Highway Research Record 255, 1968, pp. 42-58.
3. George, K. P. Cracking in Cement-Treated Bases and Means for Minimizing It. Highway Research Record 255, 1968, pp. 59-71.
4. George, K. P. Cracking in Pavements Influenced by Viscoelastic Properties of Soil-Cement. Highway Research Record 263, 1969, pp. 47-59.
5. Pretorius, P. C. The Application of the Finite Element Method of Analysis to the Design of Pavements. Department of Civil Eng., Univ. of California, Berkeley, Res. Rept. CE 299, 1968.
6. Pretorius, P. C. Design Considerations for Pavements Containing Soil-Cement Base. Univ. of California, Berkeley, PhD dissertation, 1970.
7. Wilson, E. L. Analysis of Prismatic Solids. Department of Civil Eng., Univ. of California, Berkeley, unpublished, 1967.